Human Exposure to Radio Base-Station Antennas in Urban Environment

Paolo Bernardi, *Fellow, IEEE*, Marta Cavagnaro, Stefano Pisa, *Member, IEEE*, and Emanuele Piuzzi

***Abstract*—In this paper, the human exposure to the electromagnetic field radiated by a radio base-station antenna operating around 900 MHz in an urban environment has been analyzed. A hybrid ray-tracing/finite-difference time-domain (FDTD) method has been used to evaluate the incident field and the power absorbed in an exposed subject in the presence of reflecting walls. The base-station antenna has been characterized by means of its radiation pattern, evaluated with an FDTD analysis of a typical panel antenna. Three particular situations for a rooftop mounted antenna have been considered. In all the examined cases, the obtained results, in terms of incident field and absorbed power, are below the most recognized safety standard levels. The importance of an accurate modeling of the environment in which the exposure takes place has been evidenced.**

***Index Terms*—Dosimetry, FDTD methods, human exposure, land mobile radio cellular systems, ray tracing.**

I. Introduction

THE rapid diffusion of wireless communication systems, such as cellular phones and wireless local area networks (WLANs), has caused an increased concern for the potential detrimental effects on human health deriving from exposure to electromagnetic (EM) fields emitted by the antennas of these systems.

In particular, with reference to cellular telecommunication systems, two different exposure conditions are present. The first is the exposure of the user's head to the portable phone and the second is the general population exposure to the field radiated by the base-station antennas. The power absorbed inside the head of a cellular phone user, due to the field radiated by the phone antenna, has been extensively studied (e.g., [1]–[5]), while the assessment of the human exposure to the field radiated by radio base-station antennas operating in urban areas is a task that today remains still unresolved. In fact, up to now, the exposure to base-station antennas has been studied only with reference to simplified conditions (uniform plane-wave incidence) [6]–[8]. Base stations, however, often operate in an urban environment, where many scattering objects are present (ground, buildings, etc.); therefore, the exposure conditions are quite different from free-space far-field exposure, and the need of an accurate modeling of the real scenario arises [9]. These studies are particularly important in view of the fact that people can be exposed to the field radiated by base stations for a long time, although the exposure levels are generally lower than those due to mobile terminals.

Manuscript received November 10, 1999; revised May 3, 2000.

The authors are with the Department of Electronic Engineering, University of Rome "La Sapienza," 00184 Rome, Italy.

Publisher Item Identifier S 0018-9480(00)09690-3.

At present, the most used technique for studying the power absorbed in a subject exposed to EM fields is the finite-difference time-domain (FDTD) method [10]–[12]. However, when exposure in an urban environment has to be modeled, the FDTD is not easily applicable due to the huge dimensions of the region to be studied with respect to the typical wavelength used in cellular telecommunication systems.

In this paper, the exposure of an anatomical model of the human body to the field radiated by a base-station antenna operating around 900 MHz has been studied by using a hybrid ray-tracing/FDTD technique. This technique uses the FDTD method to study a limited region just containing the exposed subject, and geometrical optics to model the field propagation in the remaining part of the domain, including the radiating antenna and the reflecting/scattering objects. The radiation pattern of the base-station antenna, which is the input of the hybrid method, has been computed by means of an FDTD analysis. Three typical exposure conditions for a rooftop mounted antenna have been considered and analyzed.

II. Methods and Models

The FDTD method is currently the most used technique in EM dosimetry problems. In fact, it allows a sufficiently accurate simulation of the field source (antenna) and a simple modeling of heterogeneous scatterers of complex shape (human body). This method, however, is not efficient to study scattering problems involving large regions (urban environment) due to the huge memory and CPU time requirements. In order to overcome this problem, in this paper, the FDTD method has been used in conjunction with the ray-tracing technique, which is able to model field propagation in large multireflection environments very efficiently.

As a first step, the ray-tracing approach is used to evaluate the EM field incident on the exposed subject, starting from the radiation pattern of the base-station antenna and taking into account reflecting walls present in the environment (buildings, ground, etc.). The ray-tracing algorithm used for the incident field evaluation is based on geometrical optics [13] and models only first-order reflections. Neglecting higher order reflections is a reasonable approximation for the particular environments that will be studied in the following; in fact, urban environments are only partially closed and the walls reflect less than 50% of the incident power. As a consequence, higher order reflections influence the field distribution only in a slight manner, and they cannot significantly alter the exposure conditions. The reflected field is evaluated by using image theory [14], characterizing each wall through its permittivity and conductivity values, and

using the well-known reflection coefficients for parallel and perpendicular polarization [15].

As a second step, the incident field obtained with ray tracing is used as an excitation inside the FDTD region in which the exposed subject is modeled, making use of the equivalence principle.

According to this principle, the total EM field present inside a limited region containing scattering objects, and due to external sources, is computed neglecting these sources and imposing equivalent electric $(\mathbf{J_e})$ and magnetic $(\mathbf{J_m})$ currents at the boundary surface of the region. In particular, considering only the scattered field to be present out of the considered region, the equivalent currents are given by

$$\mathbf{J_e} = -\mathbf{n} \times \mathbf{H_i} \tag{1}$$

$$\mathbf{J_m} = \mathbf{n} \times \mathbf{E_i} \tag{2}$$

where $\mathbf{E_i}, \mathbf{H_i}$ represent the incident field, and $\mathbf{n}$ is the unit vector normal to the boundary surface and directed toward the external (scattered field) region.

Within the hybrid method, the equivalence principle is applied dividing the FDTD domain under study in two regions: an inner region where the total EM field is computed, and an external one where only the scattered field is evaluated. This external region is then closed applying a five-cell uniaxial perfectly matched layer (UPML) absorbing boundary condition with linear profile and 1% reflection coefficient [16]. The FDTD field excitation is realized by imposing the equivalent currents (1) and (2) at the boundary surface between the two regions. The incident field $\mathbf{E_i}, \mathbf{H_i}$ required for the $\mathbf{J_e}$ and $\mathbf{J_m}$ evaluation is that computed with the ray-tracing algorithm.

Applying the proposed hybrid technique, attention must be paid to two aspects. First, the ray-tracing algorithm makes use of the radiation pattern of the source. This approach gives reliable predictions of the EM-field values only in the Fraunhofer region of the antenna, which starts at a distance from the antenna approximately equal to D^2/λ (where D is the maximum antenna dimension); this is the minimum distance at which the exposed subject can be placed. Second, the reflecting walls are modeled in the ray-tracing algorithm, but not in the FDTD one. This means that the interaction between the walls and field scattered by the exposed subject is not considered. This approximation gives rise to an error in the evaluation of power absorption, which is negligible when the exposed subject is sufficiently far from the walls. In case of exposure near reflecting walls, this approximation instead corresponds to neglecting the shadowing effect, due to losses in the exposed subject, on the image source. As a consequence, the absorbed power is overestimated, giving rise to a worst-case condition.

The radiation pattern utilized in the ray-tracing computations has been obtained through an FDTD analysis at 947.5 MHz (central frequency of the global system for mobile communications (GSM) base-station transmit band [17]) of a typical panel antenna. The considered antenna is depicted in Fig. 1 and consists of four parallel pairs of vertical dipoles, aligned on a vertical axis with a uniform spacing of 32 cm (measured at the feeding point). The horizontal spacing of the dipoles is equal to 9 cm. All dipoles are fed with equal amplitude and phase. At the back of this array is mounted (at a distance of 7 cm) a metallic flat reflector whose dimensions are 25 × 129 cm. The antenna three-dimensional radiation pattern has been obtained applying a near-to-far-field transformation to the near field evaluated by means of an FDTD analysis [10]. Fig. 2 shows the section of the obtained normalized radiation pattern on the vertical plane containing the maximum gain direction. The obtained patterns compare well with those of typical panel antennas available on the market. In particular, the −3-dB aperture on the horizontal plane is equal to about 80°, while a −3-dB aperture of 13° is obtained on the vertical plane; the overall gain of the antenna is 14.7 dBi. Usually, in order to optimize cell coverage, these antennas are mounted with a tilting angle of about 8° on the vertical plane (mechanical tilting). Therefore, the obtained three-dimensional radiation pattern has been tilted by an angle of 8°, in order to approach the realistic use condition.

To study the interaction of the radiated EM field with an exposed subject, a heterogeneous model of man has been used. This model has been obtained from a tissue-classified version

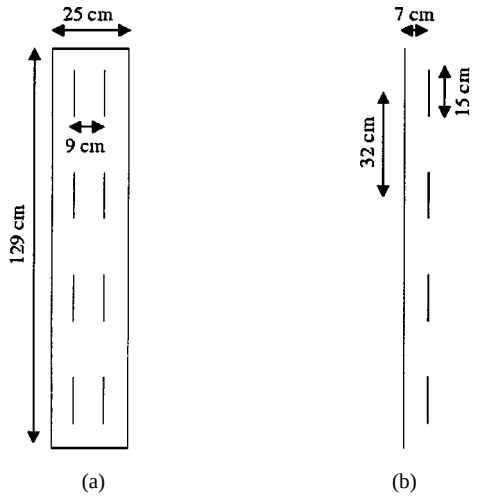

Fig. 1. Panel antenna geometry. (a) Frontal view. (b) Lateral view.

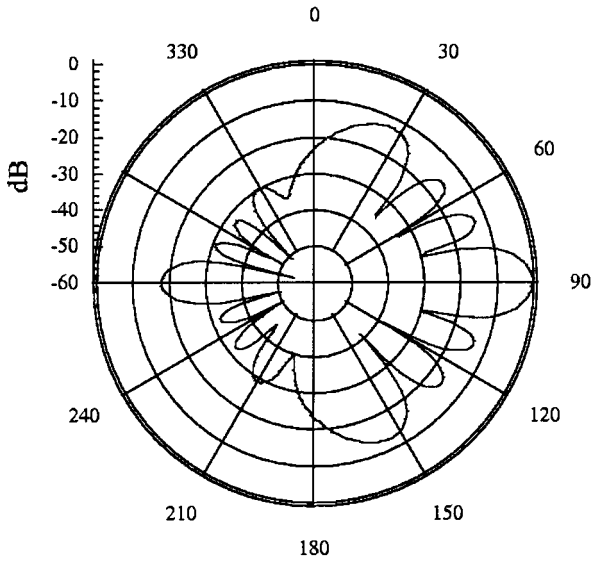

Fig. 2. Section of the antenna normalized radiation pattern on the vertical plane containing the maximum gain direction.

of the "Visible Human Project" data set1 developed at Brooks Air Force Base Laboratories, Brooks AFB, TX [18]. The original model had a 1-mm resolution and has been downsampled to obtain a final resolution of 5 mm. At the considered frequency of 947.5 MHz, in the tissue with the highest permittivity, this cell dimension corresponds to about one-tenth of the wavelength, resulting in a good accuracy for the FDTD simulations. The body model has a total height of 180 cm and 31 different types of tissues/organs have been evidenced. In particular, due to the cell dimension used, the most external layer of the model has been associated with an average tissue made of 1/2 skin and 1/2 fat. For the electrical characterization of the tissues at the considered frequency, the data reported in [19] and [20] have been used.

III. Results and Discussion

The above-described hybrid method has been used to evaluate the exposure of a subject to the field radiated by a rooftop mounted base-station antenna. Three typical exposure conditions have been considered (see Fig. 3). In all cases, the antenna is that described in the previous section, and is positioned with a mechanical tilting of 8° on the top of a 6-m-high trestle. The radiated power is 30 W, corresponding to a typical value for a four-transmitter base station in urban area. The dimensions of the FDTD total field region, in which the exposed subject is inserted, are $44 \times 69 \times 190$ cm. The human body model is facing the antenna and is kept at a height of 1 cm above the ground to take into account the effect of shoe soles. In the first situation (case I), the subject stands on the building roof, where the antenna is mounted, at a distance of 8 m from the trestle [see Fig. 3(a)]. The chosen distance is the minimum allowing the use of the Fraunhofer region approximation for the considered antenna. The subject is placed within the beam of the first lateral lobe of the radiation pattern. The roof electrical parameters are $\varepsilon_r = 5.0$ and $\sigma = 0.04$ S/m [21]. In the second situation (case II), the subject stands on a balcony in front of the building where the antenna is mounted at a distance of 30 m [see Fig. 3(b)]. The subject position corresponds to the direction of the principal lobe of the antenna. The electrical parameters for the walls are the same considered in case I. In the third situation (case III), the subject stands on the street beneath the building (30-m high) where the antenna is mounted, and another building is present at his back [see Fig. 3(c)]. The subject is positioned within the beam of the last lateral lobe of the radiation pattern. The ground electrical parameters are $\varepsilon_r = 2.0$ and $\sigma = 0.001$ S/m [22], while the building wall parameters are the same previously considered.

Table I shows the results obtained for the three examined exposure conditions. The first two columns report the spatial maximum (E_{IMAX}) and spatial average (E_{IAVE}) of the electric field rms value over the entire FDTD total field domain when the subject is not present (incident field). The last three columns refer to the case when the subject is present and report the maximum specific absorption rate (SAR) (power absorbed per unit mass) averaged over 1 g ($\mathrm{SAR}_{1\,\mathrm{g}}$), and over 10 g ($\mathrm{SAR}_{10\,\mathrm{g}}$), and the SAR averaged over the whole body (SAR_{WB}). The $\mathrm{SAR}_{1\,\mathrm{g}}$ values have been computed considering a cube with a volume of 1 cm^3 corresponding to eight FDTD cells. Only cubes weighing at least 0.9 g have been examined. As concerns the $\mathrm{SAR}_{10\,\mathrm{g}}$ values, a cube with a volume of 10 cm^3 has been considered. This volume has been obtained starting from an inner cube made of 64 FDTD cells (8 cm^3) and adding an external shell of 2 cm^3 realized with a fraction of the FDTD cells surrounding the inner cube. In this case, only cubes weighing at least 9 g have been examined.

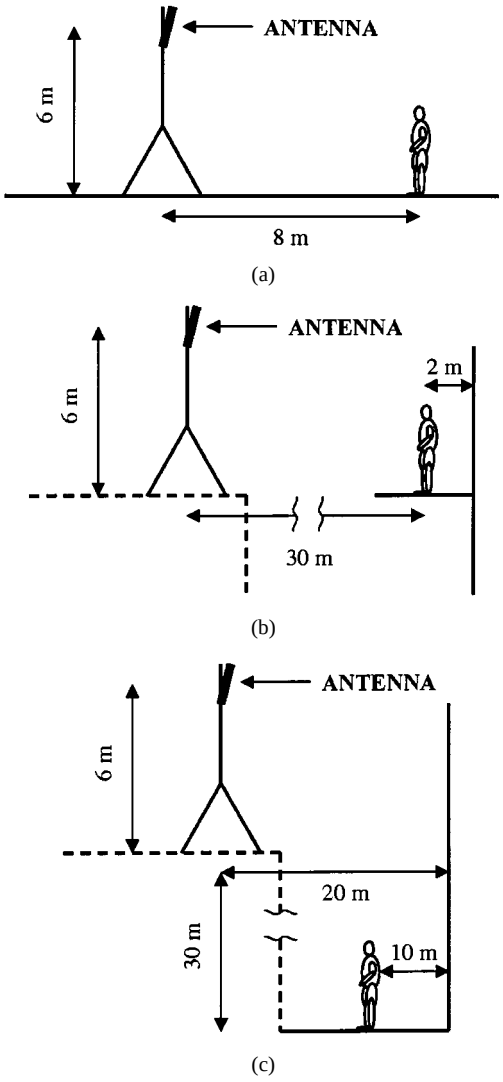

Fig. 3. Environment geometry for the three cases studied. Dashed lines represent planes not considered in the simulations. (a) Case I: subject on the building roof. (b) Case II: subject on the balcony. (c) Case III: subject on the street.

TABLE I
Spatial Maximum (E_{IMAX}), and Spatial Average (E_{IAVE}), of the Incident Field rms Value; Maximum SAR Values Averaged Over 1 g ($\mathrm{SAR}_{1\,\mathrm{g}}$), Over 10 g ($\mathrm{SAR}_{10\,\mathrm{g}}$), and SAR Value Averaged Over the Whole Body ($\mathrm{SAR}_{\mathrm{WB}}$) for the Three Exposure Conditions Considered

	E_{IMAX} (V/m)	E_{IAVE} (V/m)	SAR_{1g} (mW/kg)	SAR_{10g} (mW/kg)	$\mathrm{SAR}_{\mathrm{WB}}$ (mW/kg)
Case I	4.2	2.8	5.3	3.0	0.12
Case II	8.1	5.5	13.2	8.5	0.46
Case III	1.3	1.1	0.26	0.17	0.01

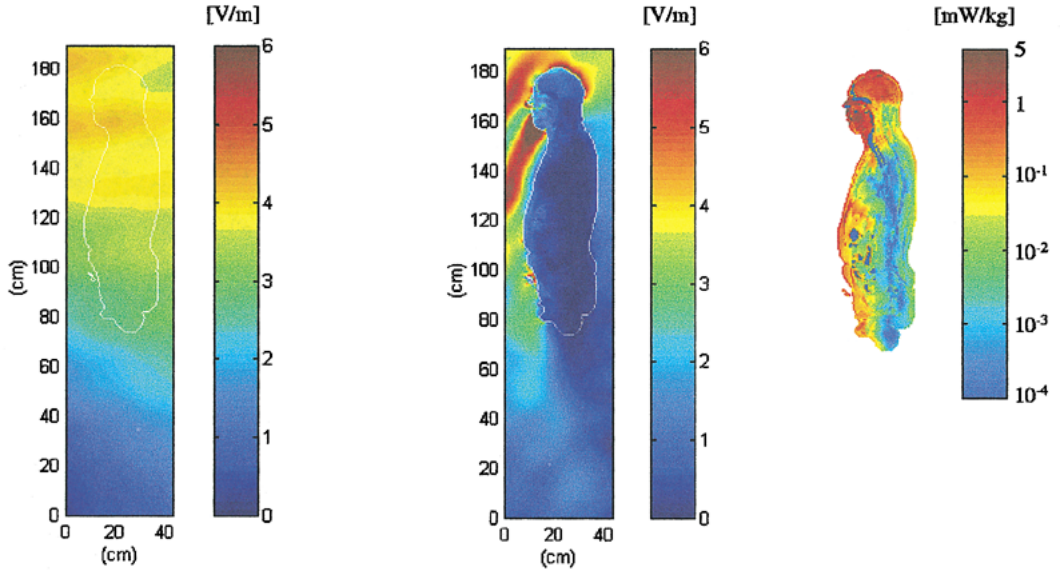

Fig. 4. Case I: electric field rms amplitude ($E_{\rm rms}$) and SAR distributions on the vertical plane containing the antenna maximum radiation direction. (a) $E_{\rm rms}$ when the subject is absent. (b) $E_{\rm rms}$ when the subject is present. (c) SAR inside the subject.

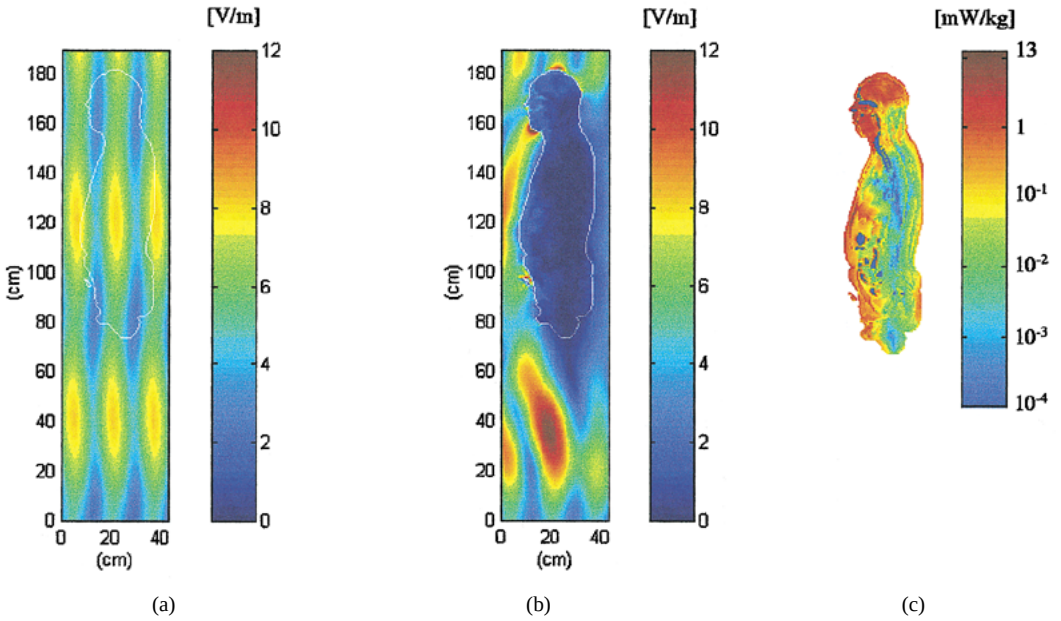

Fig. 5. Case II: electric field rms amplitude ($E_{\rm rms}$) and SAR distributions on the vertical plane containing the antenna maximum radiation direction. (a) $E_{\rm rms}$ when the subject is absent. (b) $E_{\rm rms}$ when the subject is present. (c) SAR inside the subject.

From Table I, it appears that, due to the high directivity on the vertical plane of the base-station antenna considered, the highest field levels are not obtained on the roof of the building where the antenna is located, but rather on the nearby building placed in the direction of the maximum antenna radiation. The differences between maximum and average values (up to 50% in cases I and II) evidence the nonuniformity of the field distribution. As expected, the lowest field levels are experienced by the subject standing in the street due to the high distance from the antenna and to the angled position with respect to the antenna pointing direction.

The obtained results, both in terms of incident field and SAR values, can be compared with reference levels and basic limits proposed in the main international protection standards [23]–[26]. The field values ($E_{\rm IMAX}, E_{\rm IAVE}$) in Table I are well below the safety levels reported in the standards, which, at the frequency of 947.5 MHz, are 48.7 [23], [24] and 42.3 V/m [25], [26]. As concerns the SAR, all the considered safety standards recommend a basic limit on the $\rm SAR_{WB}$ of 0.08 W/kg, while limits on local SAR are 1.6 W/kg averaged over 1 g [23], [24] or 2.0 W/kg averaged over 10 g [25], [26]. A glance at Table I shows that all the computed SAR values are at least two order of magnitude lower than the above cited limits.

The field and SAR distributions obtained in the three considered situations are shown in Figs. 4(a)–(c)–6(a)–(c). Each figure shows the distribution of the rms amplitude of the electric field

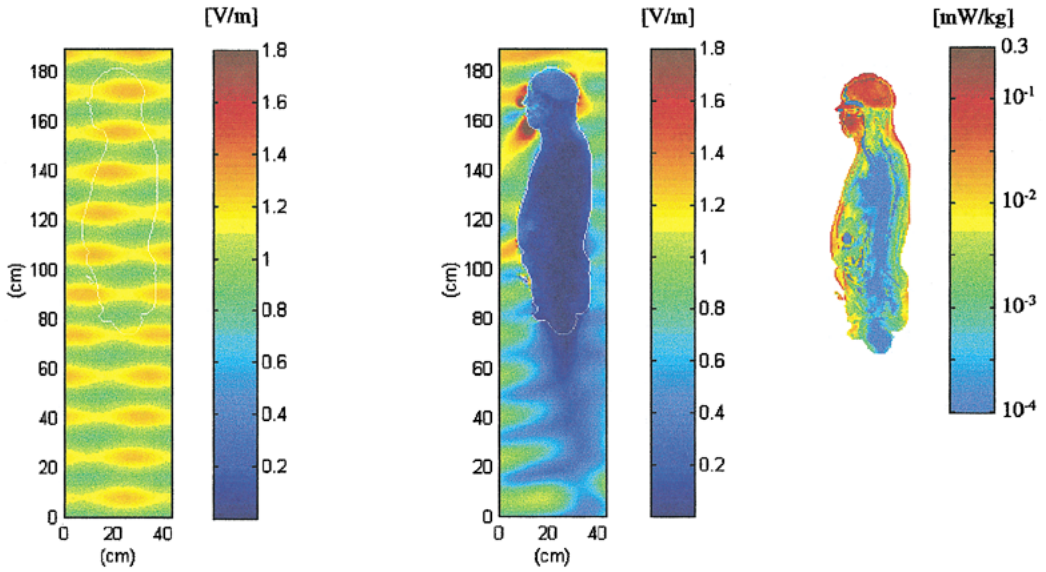

Fig. 6. Case III: electric field rms amplitude ($E_{\rm rms}$) and SAR distributions on the vertical plane containing the antenna maximum radiation direction. (a) $E_{\rm rms}$ when the subject is absent. (b) $E_{\rm rms}$ when the subject is present. (c) SAR inside the subject.

on the vertical plane containing the antenna maximum radiation direction: (a) in the absence of the subject, (b) in the presence of the subject, and (c) the SAR distribution inside the subject in the same plane. In Figs. 4(a)–6(a), the position where the subject will be placed is outlined. The field distributions when the subject is absent [see Figs. 4(a)–6(a)] reflect both the position of the examined area with respect to the antenna and the characteristics of the surrounding environment. In Fig. 4(a), the secondary lobe of the antenna, together with the vertical interference pattern due to roof reflections, are clearly evident. Figs. 5(a) and 6(a) show the presence of vertical and horizontal interferences resulting from the two orthogonal reflecting surfaces. Figs. 4(b)–6(b) show the strong alterations that the field undergoes when the subject is present. The analysis of the SAR distributions reported in Figs. 4(c)–6(c) shows that the power absorption characteristics vary considerably in the three considered cases. In case I, absorption takes place mainly in the head and chest [see Fig. 4(c)], which are directly exposed to the radiated field. In case II, significant absorption takes place also in the back of the subject [see Fig. 5(c)] due to the reflections coming from the rear building wall. Case III is the one in which absorption is more confined, being mainly limited to the head region [see Fig. 6(c)] due to the antenna positioning with respect to the exposed subject and to the low ground reflections.

In order to better identify the power absorbed inside the main body organs, the SAR values averaged over 1 g ($\rm SAR_{1\,g}$), 10 g ($\rm SAR_{10\,g}$), and the organ whole mass ($\rm SAR_{WO}$) are reported in Table II.

Results obtained for case I show that power absorption is mainly confined to the organs placed in the upper part of the body. This kind of behavior is strictly correlated to the characteristics of the incident field that, as already shown, impinges essentially on the head region [see Fig. 4(a)]. In case II, power absorption is instead distributed more uniformly among the different body organs. In all cases, the SAR values computed in the various body organs are well below the peak values reported in Table I. In fact, body organs are generally protected by tissue layers, such as skin and muscle, where most of the power is absorbed.

TABLE II
MAXIMUM SAR VALUES AVERAGED OVER 1 g ($\rm SAR_{1\,g}$), OVER 10 g ($\rm SAR_{10\,g}$), AND OVER THE WHOLE MASS ($\rm SAR_{WO}$) OF THE MAIN BODY ORGANS FOR THE THREE EXPOSURE CONDITIONS CONSIDERED

	CASE I			CASE II			CASE III		
	$\rm SAR_{1g}$	$\rm SAR_{10g}$	$\rm SAR_{WO}$	$\rm SAR_{1g}$	$\rm SAR_{10g}$	$\rm SAR_{WO}$	$\rm SAR_{1g}$	$\rm SAR_{10g}$	$\rm SAR_{WO}$
Brain	1.38	0.72	0.33	2.71	1.40	0.63	0.13	0.07	0.04
Eyes	1.67	-	1.27	3.44	-	2.45	0.07	-	0.06
Heart	0.39	0.21	0.06	1.57	0.82	0.21	0.02	0.01	<
Kidney	0.04	0.01	<	0.13	0.03	0.03	<	<	<
Liver	0.51	0.27	0.05	1.42	0.79	0.17	0.03	0.02	<
Pancreas	0.10	-	0.03	0.35	-	0.10	0.01	-	<
Spleen	0.06	0.01	0.01	0.14	0.07	0.04	0.01	<	<
Testis	0.80	-	0.41	2.31	-	1.10	0.04	-	0.02

SAR is in mW/kg.
"<" means less than 0.01.

A relevant point is the influence of the environment on incident field levels and power absorption. To get some insight into this issue, the simulations performed for case II, which is the "worst case," have been repeated neglecting the presence of the two reflecting walls (free-space condition—case $\rm II_{fr}$). The $E_{\rm IMAX}$ and $E_{\rm IAVE}$ values found are 5.4 and 5.3 V/m, respectively. These new values, compared with those previously evaluated (see Table I, second row), show that the field distribution becomes more uniform with the maximum field level decreasing by about 33%, while the average value remains almost unchanged. The SAR values evaluated in case $\rm II_{fr}$ are $\rm SAR_{1\,g} = 12.9$ mW/kg, $\rm SAR_{10\,g} = 8.2$ mW/kg,

and $\mathrm{SAR_{WB}} = 0.41$ mW/kg. These results, compared with those obtained in case II, show that both the average field level and SAR values remain almost unchanged. It must be noted, however, that this result is dependent upon the dielectric characteristics of the building walls that give rise to rather low reflections (reflection coefficients not higher than 0.4). In fact, considering a reflection coefficient of 0.7, the presence of the reflecting walls results in a 40% increase in the average field levels with a corresponding doubling in the $\mathrm{SAR_{WB}}$ value with respect to the free-space condition [9].

The obtained results show that an accurate modeling of the real environment can be a key factor for a correct evaluation of the exposure conditions.

IV. Conclusions

The evaluation of human exposure to new telecommunication systems, which are becoming more and more widespread, has become an important issue. In fact, these new systems usually operate in a rather complex environment where many field sources and scattering objects are present. In these situations, accurate investigations are needed to assess if human exposure can give rise to health risks and to verify if existing protection standards are still adequate.

In this paper, the exposure of a subject to the field radiated by a base-station antenna in urban environment has been studied. The exposure has been analyzed coupling the FDTD method with a ray-tracing algorithm suitable to treat field propagation in a partially closed environment.

The obtained results show the strong nonuniformity of the field distribution produced by base-station antennas in urban environment. This nonuniformity arises from both the narrow radiation pattern of typical panel antennas and from environmental reflections. Since human exposure to radio base stations usually happens in the far field of the antenna, compliance with protection standards is currently tested using incident field reference levels, which should ensure that basic limits (i.e., limits on SAR) are not exceeded. However, existing protection standards derive reference levels on the basis of uniform plane wave exposure studies; therefore, exhaustive investigations are needed to establish if (in complex exposure situations) SAR values are simply correlated to average field levels or if the presence of peaks in the field distribution can give rise to enhancements in the local SAR.

In the exposure conditions examined in this paper, incident field and SAR values well below the safety levels established by the most recognized international organizations have been found. From these results, it appears that exposure to the field radiated by base-station antennas cannot represent a risk for human health from the thermal point-of-view. However, an open issue is the possibility of long-term nonthermal effects of these fields. This problem can be addressed, for example, through epidemiological studies, which, in order to be effective, require an accurate evaluation of the internally induced field. Of course, during the day, exposed subjects are in movement and, therefore, exposure conditions vary. However, time spent in different typical places can be described statistically. Internal field levels induced in each of these places can be evaluated by using the proposed hybrid method and, hence, used for a statistical characterization of the exposure.

References

[1] P. Bernardi, M. Cavagnaro, and S. Pisa, "Evaluation of the SAR distribution in the human head for cellular phones used in a partially closed environment," *IEEE Trans. Electromag. Compat.*, vol. 38, pp. 357–366, Aug. 1996.

[2] O. P. Gandhi, G. Lazzi, and C. M. Furse, "Electromagnetic absorption in the human head and neck for mobile telephones at 835 and 1900 MHz," *IEEE Trans. Microwave Theory Tech.*, vol. 44, pp. 1884–1897, Oct. 1996.

[3] M. Okoniewski and M. A. Stuchly, "A study of the handset antenna and human body interaction," *IEEE Trans. Microwave Theory Tech.*, vol. 44, pp. 1855–1864, Oct. 1996.

[4] V. Hombach, K. Meier, M. Burkhardt, E. Kuhn, and N. Kuster, "The dependence of EM energy absorption upon human head modeling at 900 MHz," *IEEE Trans. Microwave Theory Tech.*, vol. 44, pp. 1865–1873, Oct. 1996.

[5] S. Watanabe, M. Taki, T. Nojima, and O. Fujiwara, "Characteristics of the SAR distributions in a head exposed to electromagnetic fields radiated by a hand-held portable radio," *IEEE Trans. Microwave Theory Tech.*, vol. 44, pp. 1874–1883, Oct. 1996.

[6] S. S. Stuchly, A. Kraszewski, M. Stuchly, G. Hartsgrove, and R. J. Spiegel, "RF energy deposition in a heterogeneous model of man," *IEEE Trans. Biomed. Eng.*, vol. BME-34, pp. 951–957, Dec. 1987.

[7] O. P. Gandhi, Y. Gu, J. Y. Chen, and H. I. Bassen, "Specific absorption rates and induced current distributions in an anatomically based human model for plane-wave exposure," *Health Phys.*, vol. 63, pp. 281–290, Sept. 1992.

[8] P. Bernardi, M. Cavagnaro, S. Pisa, and E. Piuzzi, "Evaluation of SAR and temperature distribution in subjects exposed in the far-field of radiating radio frequency sources," in *Proc. Int. Electromag. Compat. Symp.*, Rome, Italy, Sept. 1998, pp. 190–193.

[9] ——, "Evaluation of the power absorbed in subjects exposed to EM fields in partially closed environments by using a combined analytical-FDTD method," in *IEEE MTT-S Int. Microwave Symp. Dig.*, Anaheim, CA, June 1999, pp. 599–602.

[10] K. S. Kunz and R. J. Luebbers, *The Finite Difference Time Domain Method for Electromagnetics*. Boca Raton, FL: CRC Press, 1993.

[11] A. Taflove, *Computational Electrodynamics: The Finite-Difference Time-Domain Method*. Norwood, MA: Artech House, 1995.

[12] ——, *Advances in Computational Electrodynamics: The Finite-Difference Time-Domain Method*. Norwood, MA: Artech House, 1998.

[13] G. A. Deschamps, "Ray techniques in electromagnetics," *Proc. IEEE*, vol. 60, pp. 1022–1035, Sept. 1972.

[14] S. Y. Tan and H. S. Tan, "UTD propagation model in an urban street scene for microcellular communications," *IEEE Trans. Electromag. Compat.*, pp. 423–428, Nov. 1993.

[15] C. A. Balanis, *Advanced Engineering Electromagnetics*. New York: Wiley, 1989.

[16] S. D. Gedney, "An anisotropic perfectly matched layer-absorbing medium for the truncation of FDTD lattices," *IEEE Trans. Antennas Propagat.*, vol. 44, pp. 1630–1639, Dec. 1996.

[17] "Digital Cellular Telecommunication System, Radio Transmission and Reception," ETSI, Sophia Antipolis, France, GSM 05.05, 1996.

[18] J. M. Ziriax, D. Le Blanc, P. A. Mason, and W. D. Hurt, "Finite-difference time-domain for personal computers," in *21st BEMS Meeting*, Long Beach, CA, June 1999, p. 57.

[19] S. Gabriel, R. W. Lau, and C. Gabriel, "The dielectric properties of biological tissues: III. Parametric models for the dielectric spectrum of tissues," *Phys. Med. Biol.*, vol. 41, pp. 2271–2293, 1996.

[20] C. Gabriel, "Compilation of the dielectric properties of body tissues at RF and microwave frequencies," Brooks Air Force, Brooks AFB, TX, Tech. Rep. AL/OE-TR-1996-0037, 1996.

[21] M. Barbiroli, C. Carciofi, G. Falciasecca, and M. Frullone, "Analisi dell'irradiazione elettromagnetica nei pressi di stazioni base GSM—Parte B: Valutazione del campo," in *Proc. AEI Environmental Impact Electromagn. Fields Workshop*, Roio, Italy, July 1998, pp. 29–34.

[22] P. Daniele, V. Degli Esposti, G. Falciasecca, and G. Riva, "Strumenti per la previsione di campo in ambito microcellulare outdoor e indoor," *Alta Freq.*, vol. 6, pp. 112–115, Nov.–Dec. 1994.

[23] *IEEE Standard for Safety Levels with Respect to Human Exposure to Radio Frequency Electromagnetic Fields, 3 kHz to 300 GHz*, IEEE Standard C95.1–1991, 1992.
[24] "Evaluating compliance with FCC guidelines for human exposure to radiofrequency electromagnetic fields," Federal Commun. Commission, Washington, DC, OET Bulletin 65, Aug. 1997.
[25] *Human Exposure to Electromagnetic Fields. High Frequency (10 kHz to 300 GHz)*, European Communities Prestandard ENV 50 166-2, Jan. 1995.
[26] ICNIRP, "Guidelines for limiting exposure to time-varying electric, magnetic, and electromagnetic fields (up to 300 GHz)," *Health Phys.*, vol. 74, no. 4, pp. 494–522, 1998.

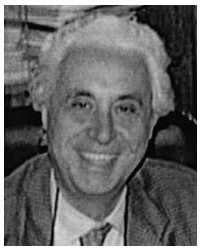

Paolo Bernardi (M'66–SM'73–F'93) was born in Civitavecchia, Italy, in 1936. He received the electrical engineering degree and Libera Docenza degree from the University of Rome, Rome, Italy, in 1960 and 1968, respectively.

Since 1961, he has been with the Department of Electronics, University of Rome "La Sapienza," Rome, Italy, where he became a Full Professor in 1976 and was Director of the Department from 1982 to 1988. His research has dealt with the propagation of EM waves in ferrites, microwave components, biological effects of EM waves, and EM compatibility. He has authored over 150 scientific papers and numerous invited presentations at international workshops and conferences. He was chairman of the URSI Commission K on Electromagnetics in Biology and Medicine (1993–1996), chairman of a Commission of the Italian National Research Council (CNR) working on a National Project on Electromagnetic Compatibility in Electrical and Electronic Systems, vice-chairman of the European Community COST Project 244 on Biomedical Effects of Electromagnetic Radiation (1993–1997), and project coordinator of the European Community Project CEPHOS, which is devoted to EM dosimetry and compliance with standards of mobile cellular phones. He is an associate editor for the URSI *Radio Science Bulletin*. He was an Editorial Board member of *Microwave And Optical Technology Letters*. He was the guest editor of special issues on "Nonionizing Electromagnetic Radiation" of *Alta Frequenza* (March 1980) and "Exposure Hazards and Health Protection in Personal Communication Services"of *Wireless Networks* (December 1997).

Dr. Bernardi is a member of the Bioelectromagnetics Society (BEMS), European Bioelectromagnetics Association (EBEA), and "Socio Fedele" of the Italian Electrical and Electronic Society (AEI). From 1979 to 1980, he was the chairman of the IEEE Middle and South Italy Sections. He was an Editorial Board member for the IEEE TRANSACTIONS ON MICROWAVE THEORY AND TECHNIQUES. He was the recipient of the 1984 IEEE Centennial Medal.

Marta Cavagnaro was born in Rome, Italy, in 1966. She received the Electronic Engineering degree (*cum laude*) and the Ph.D. degree from the University "La Sapienza" of Rome, Rome, Italy, in 1993 and 1997, respectively.

Her current research interests are dosimetric aspects of the interaction between EM fields and biological systems, and numerical techniques.

Dr. Cavagnaro was the recipient of an Alenia Spazio S.p.A. Scholarship to study the coupling between EM fields and triaxial cables. She was also the recipient of the 1996 URSI Young Scientist Award.

Stefano Pisa (M'91) was born in Rome, Italy, in 1957. He received the Electronic Engineering and Ph.D. degrees from the University "La Sapienza" of Rome, Rome, Italy, in 1985 and 1988, respectively.

He is currently a Researcher with the Department of Electronic Engineering, University "La Sapienza" of Rome. His research interests are in the interaction between EM fields and biological systems and in therapeutic and diagnostic applications of EM fields.

Emanuele Piuzzi was born on May 25, 1972 in Lecce, Italy. He received the Electronic Engineering degree (*cum laude*) from the University "La Sapienza" of Rome, Rome, Italy, in 1997, and is currently working toward the Ph.D. degree at the University "La Sapienza" of Rome.

He is currently studying hybrid techniques for the solution of Maxwell's equations, with particular attention to those involving FDTD. His research interests are RF dosimetry, heating induced inside human beings exposed to RF and microwave fields, and hybrid numerical techniques for EM- field computation.